Hydraulic integration and shrub growth form linked across continental aridity gradients

H. Jochen Schenk*†, Susana Espino*, Christine M. Goedhart*‡, Marisa Nordenstahl§¶, Hugo I. Martinez Cabrera‖, and Cynthia S. Jones‖

*Department of Biological Science, California State University, Fullerton, CA 92834-6850; §Facultad de Agronomía, Universidad de Buenos Aires, C1417DSE Buenos Aires, Argentina; and ‖Department of Ecology and Evolutionary Biology, University of Connecticut, Storrs, CT 06269-3043

Communicated by William H. Schlesinger, The Institute of Ecosystem Studies, Millbrook, NY, May 19, 2008 (received for review November 14, 2007)

Both engineered hydraulic systems and plant hydraulic systems are protected against failure by resistance, reparability, and redundancy. A basic rule of reliability engineering is that the level of independent redundancy should increase with increasing risk of fatal system failure. Here we show that hydraulic systems of plants function as predicted by this engineering rule. Hydraulic systems of shrubs sampled along two transcontinental aridity gradients changed with increasing aridity from highly integrated to independently redundant modular designs. Shrubs in humid environments tend to be hydraulically integrated, with single, round basal stems, whereas dryland shrubs typically have modular hydraulic systems and multiple, segmented basal stems. Modularity is achieved anatomically at the vessel-network scale or developmentally at the whole-plant scale through asymmetric secondary growth, which results in a semiclonal or clonal shrub growth form that appears to be ubiquitous in global deserts.

plant hydraulic systems | wood anatomy | hydraulic redundancy | xylem structure and function

In engineering terms, the hydraulic system of a plant is a negative-pressure flow system. This type of hydraulic system, whether natural or man-made, is prone to fail when air bubbles (emboli) are introduced, because under strong negative pressure a single embolism can lead to breakage of the water column unless the air bubble is isolated in a branch or pipe. Both drought and freezing can cause embolisms in plants (1).

Drought-induced embolisms form under negative pressure, when air is pulled into a water-filled conduit from adjacent air-filled spaces or cells, a process known as "air seeding." This common, even daily, event (2–4) can lead to complete failure of the hydraulic system if runaway embolism occurs (5). Two of the three attributes by which plants' negative-pressure flow systems can be protected against failure, resistance and reparability, have been subjects of active research during the last decade (2–4, 6–10). The third attribute, redundancy, has received much less attention as an important drought adaptation but is emerging as a focus of research (11–14). Attributes of redundancy in hydraulic systems of vessel-bearing angiosperms include the numbers of vessels (14), the vessel network topology (12), the number and sizes of pits between adjacent vessels (13, 15, 16), and the division of whole plants into independent hydraulic units (17).

A basic rule of reliability engineering states that the level of independent redundancy should increase with increasing risk of fatal system failure (18); hydraulic engineers routinely increase the safety of man-made pressure-flow systems by designing them to be redundant (19). Redundancy in hydraulic systems (Fig. 1) can vary from a high degree of inter-connectedness (i.e., integrated redundancy) to complete, independent compartmentation (i.e., modular redundancy). In a negative-pressure flow system, integrated redundancy allows alternate water transport pathways around blockages of individual conduits (caused by pathogens or tyloses in plants), while leaving the system vulnerable to runaway embolisms. Only modular redundancy can restrict embolisms to a single conduit or group of conduits;

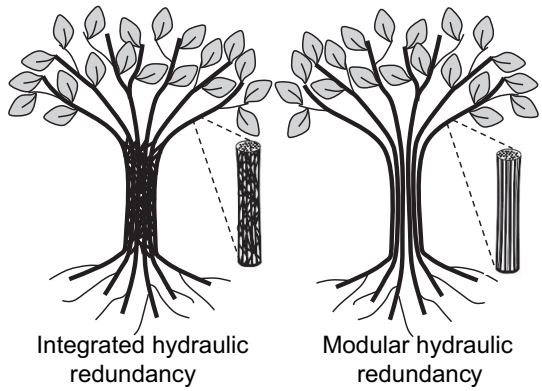

Fig. 1. Integrated and modular hydraulic systems in plants at the level of whole plants and individual stems. Dark lines illustrate pathways of water transport.

therefore modular redundancy may be expected to be a common trait in plants that face increased risk of hydraulic failure caused by drought (11).

Division of plant hydraulic systems into independent hydraulic modules has been reported for a number of shrub species in which asymmetric secondary growth resulting from unequal cambial activity leads to deep segmentation of stems, causing a functional division of the water-conducting sapwood into independent hydraulic modules (17, 20). In some species, stems remain physically connected by nonconducting heartwood (21); others split axially along woody stems and roots into physically separate plants (Fig. 2) (17, 22, 23). Many dominant shrub genera in the world's deserts, *Artemisia*, *Ambrosia*, *Larrea*, and *Salsola*, have this growth form (17). Modular hydraulic redundancy also can be conferred anatomically by reduced vessel contact or lack of intervessel pitting (11, 24) and by isolation of vessels or vessel groups in a fiber matrix (25). Water-filled libriform fibers and fiber tracheids can conduct water (26), but their conductivity is likely to be extremely low and is likely to be zero if they are filled with gas, as has been shown to occur in several tree species (27–29). Anatomical traits that reduce lateral water flow among neighboring vessels or groups of vessels reduce the ratio of tangential and/or radial to axial water flow (11, 24, 30) and result in sectorial patterns of water ascent (31).

Author contributions: H.J.S., H.I.M.C., and C.S.J. designed research; H.J.S., S.E., C.M.G., M.N., H.I.M.C., and C.S.J. performed research; H.J.S., S.E., and H.I.M.C. analyzed data; and H.J.S. and C.S.J. wrote the paper.

The authors declare no conflict of interest.

†To whom correspondence should be addressed. E-mail: jschenk@fullerton.edu.

‡Present address: Department of Ecology & Evolutionary Biology, University of California, Irvine, CA 92697-2525.

¶Present address: Department of Biological Sciences, Macquarie University, Sydney, NSW 2109, Australia.

This article contains supporting information online at www.pnas.org/cgi/content/full/0804294105/DCSupplemental.

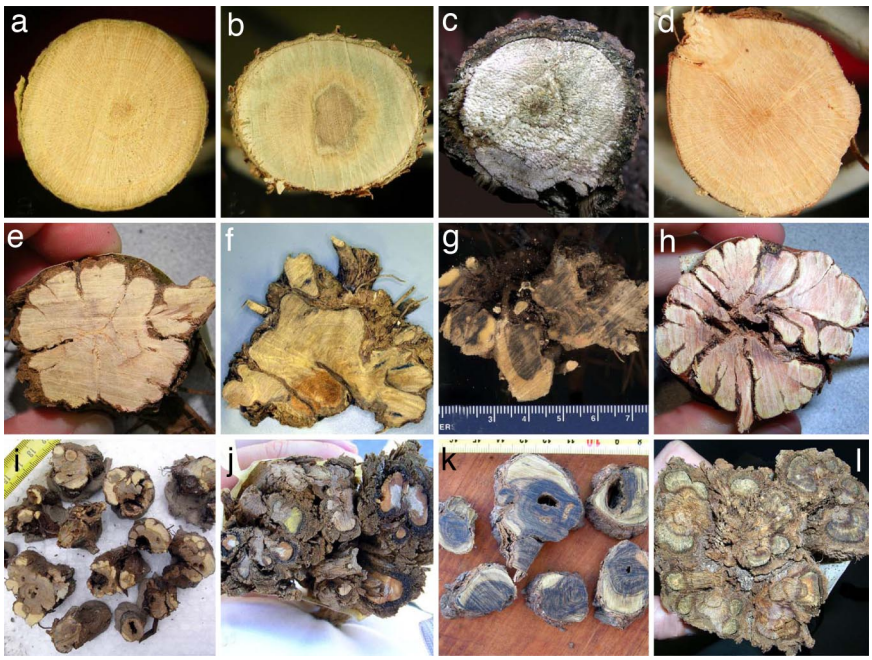

Fig. 2. Representative examples of basal stem shapes for 12 shrub species from North and South America. Stem segmentation indices $S = perimeter/(\sqrt{area}2\sqrt{\pi})$ are listed in parentheses. (*a*) *Rhus glabra* (1.07), Whitehall. (*b*) *Ilex mucronata* (1.10), Coweeta. (*c*) *Baccharis spicata* (1.11), El Palmar. (*d*) *Vaccinium arboretum* (1.14), Whitehall. (*e*) *Salvia mellifera* (2.30), Tucker. (*f*) *Lippia turbinata* (1.42), Cruz de Piedra. (*g*) *Dalea formosa* (2.66), Copper Breaks. (*h*) *Eriogonum fasciculatum* (2.84), Tucker. (*i*) *Junellia aspera* (4.70), La Tranca. (*j*) *Ambrosia dumosa* (4.39), Desert Center. (*k*) *Larrea divaricata* (3.81), Talacasto. (*l*) *Hymenoclea salsola* (4.44), Desert Center.

To quantify the extent of hydraulic integration and its relation to growth form and morphological modularity, we studied 75 dicot shrub species along two transcontinental aridity gradients between 31° and 35° latitude in North America and South America [Table 1 and supporting information (SI) Table S1]. We characterized hydraulic integration by the degree of basal stem segmentation and the lateral spread of dye tracer in basal stems and related both to measures of growth form and wood traits.

Results and Discussion

The degree of basal stem segmentation (S) decreased with increasing mean annual precipitation (MAP) (Fig. 3*a*; Table 2), which in turn was correlated linearly with aridity (the aridity index equals MAP divided by the mean annual potential evapotranspiration; $n = 10$; $r^2 = 0.984$; $P < .0001$). The slope of the relationship between S and MAP was significantly steeper for the North American than for the South American transect (Fig. 3*a*). Stem segmentation was not strongly related to canopy volume ($n = 138$; $r^2 = 0.167$; $P = .051$) but decreased exponentially with increasing canopy height-to-width ratio ($n = 138$; $r^2 = -0.638$; $P < .0001$) and was negatively related to canopy height ($n = 138$; $r^2 = -0.308$; $P < .001$) and the height of the lowest branch above ground ($n = 90$; Wilcoxon Signed Rank Statistic $Z = -2.517$; $P = .012$). The relationship between S and MAP was significant even when MAP, shrub height, and their interaction were included as additional variables in a general linear model to account for the effects of water availability and the biomechanical requirements of taller stems ($r^2 = 0.2809$; effects: MAP, $P = .0019$; shrub height, $P = .0135$; MAP × shrub height, $P = .0399$). Of all shrub species sampled in arid to semiarid environments, 46% had completely split axes (Fig. 2) and therefore consisted of several separate physiological indi-

Table 1. Field sites in North America (United States) and South America (Argentina)

Location	Coordinates	MAP	PET	AI	Seas.	Vegetation
North America						
Desert Center, CA	33°44′ N 115°30′ W	100	1,585	0.06	W	Desert scrub
Tucker WS, CA	33°43′ N 117°37′ W	325	1,143	0.28	W	Sage scrub
Copper Breaks StP, TX	34°06′ N 99°45′ W	660	1,450	0.46	SP	Mesquite savanna
Union, SC	34°39′ N 81°57′ W	1,220	979	1.25	N	Pine forest
Whitehall EF, GA	33°57′ N 83°22′ W	1,250	1,018	1.23	N	Hardwood forest
Coweeta LTER, NC	35°03′ N 83°25′ W	1,850	900	2.06	N	Hardwood forest
South America						
Talacasto, San Juan	31°13′ S 68°39′ W	90	1,082	0.08	S	Desert scrub
La Tranca, San Luis	32°22′ S 67°10′ W	250	1,141	0.22	S	Desert scrub
Cruz de Piedra, San Luis	33°13′ S 66°14′ W	680	1,149	0.59	S	Mesquite savanna
El Palmar NP, Entre Rios	31°53′ S 58°14′ W	1,190	981	1.21	S	Palm forest

AI, aridity index MAP/PET; EF, experimental forest; MAP, mean annual precipitation; N, no pronounced seasonality; NP, national park; PET, mean annual potential evapotranspiration; S, summer maximum; Seas., seasonality of precipitation; SP, spring maximum; StP, state park; LTER, long-term ecological research site; W, winter maximum; WS, wildlife sanctuary.

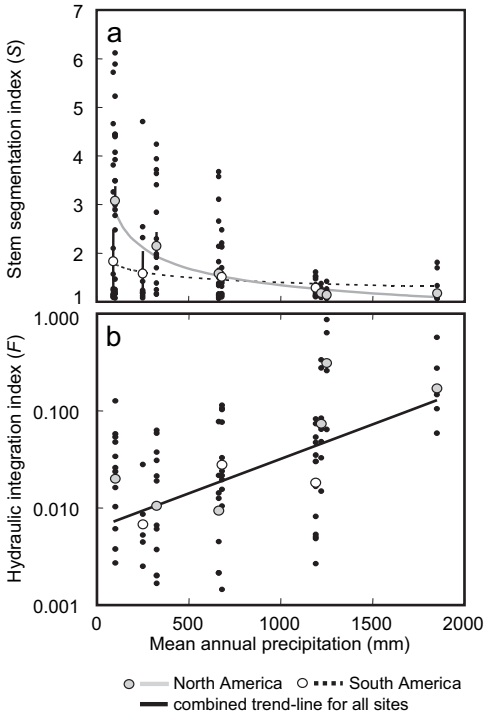

Fig. 3. Degree of hydraulic integration of shrubs as a function of mean annual precipitation (MAP). Black dots are data for individual shrubs, and large circles are geometric means for individual field sites. (*a*) Stem segmentation index *S*. Relationships for North and South America were significantly different: $n = 159$; $F_{continent} = 10.29$, degrees of freedom (d.f.) = 1, $P = .0016$; $F_{MAP} = 28.80$, d.f. = 1, $P < .0001$; $F_{continent \times MAP} = 4.41$, d.f. = 1, $P = .0373$). (*b*) Hydraulic integration index *F*. Relationships for North and South America did not differ significantly: $n = 86$; $F_{continent} = 0.68$, d.f. = 1, $P = .4103$; $F_{MAP} = 8.85$, d.f. = 1, $P = .0038$; $F_{continent \times MAP} = 2.55$, d.f. = 1, $P = .1141$).

viduals (17). In contrast, no shrubs from humid environments were completely split; rather, they tended to be single stemmed with more or less circular basal stems. Shrubs growing in the understory of humid warm-temperate forests may well be described as miniature trees, albeit with very short trunks. Shrubs between these extremes in climate tend to be intermediate in their growth forms.

The degree of hydraulic integration calculated from the lateral spread of dye in basal stem cross-sections (index *F*) also increased with MAP (Fig. 3*b*; Table 2), with no significant difference in this relationship between the North and South American transects. The relationship between *F* and MAP remained significant even when the stem area and its interaction with MAP were included in the analysis to account for the possibility that larger stems may tend to have smaller fractions of their wood colored by dye tracer ($r^2 = 0.2572$, MAP, $P < .0001$; stem area, $P = .395$: MAP × stem area, $P = .089$). Functionally, dryland shrubs tend to be much less hydraulically integrated than shrubs in humid environments.

The hydraulic integration index *F* was negatively correlated with fiber wall thickness (Table 2), especially after correction for confounding effects of fiber lumen diameters (Fig. 4), was negatively correlated with the hydraulic diameter of vessels [except for phylogenetically independent contrasts (PICs)], and was positively correlated with vessel density, as previously observed for other species (11). The stem segmentation index *S* was positively correlated with the theoretical implosion resistance of vessels $(t/b)_h^2$ and with sapwood density (Table 2), which decreased with precipitation. The stem segmentation index *S* and integration index *F* were not significantly correlated with each other ($n = 61$; $r = -0.207$; $P = .109$; PICs: $n = 52$; $r = -0.224$; $P = .088$). Stem-splitting shrubs compared with nonsplitting shrubs from dry environments (Table 3) had higher vessel densities, smaller vessel hydraulic diameters, higher wood densities, and higher vessel implosion resistance, indicating strong resistance to drought-induced embolism formation (7, 13, 32).

As predicted by principles of hydraulic engineering, the incidence and degree of hydraulic modularity in shrubs increased with increasing risk of failure resulting from drought. Hydraulic integration thus joins the list of other plant traits that have been observed to correlate with aridity, including the pubescence, sizes, shapes, mass area relationships, and life spans of leaves (33–35) and photosynthetic pathways (36). Because correlation does not prove causation, the question arises as to which factors other than adaptation to drought could explain the relationship observed between hydraulic modularity and aridity. For example, stem segmentation (Fig. 2) might result when drought leads to differential growth or partial dieback of branches, thereby

Table 2. Correlation coefficients for relationships of sapwood traits with the hydraulic integration index, stem segmentation index, and with mean annual precipitation

	Hydraulic integration index $F^{\dagger}$ ($n = 49^{\ddagger}$)		Stem segmentation index $S^{\dagger}$ ($n = 62^{\ddagger}$)		Mean annual precipitation ($n = 62^{\ddagger}$)	
Trait	Uncorr.	PIC	Uncorr.	PIC	Uncorr.	PIC
Vessel density†	0.513**	0.413*	0.114	0.024	0.068	−0.161
Vessel hydraulic diam.	−0.361*	−0.293	−0.210	−0.178	−0.128	−0.021
Fiber wall thickness	−0.495**	−0.434*	0.051	0.303	0.122	0.058
Fiber lumen diam.	−0.092	−0.208	−0.169	−0.083	0.483***	0.378*
$FWTI_{\%}$	−0.534***	−0.559***	0.205	0.327*	−0.220	−0.247
Fiber wall area, %	−0.088	−0.000	0.269	0.195	−0.366*	−0.299
Fiber lumen area, %	0.094	−0.051	−0.229	−0.141	0.470**	0.364*
$(t/b)_h^2$	−0.163	−0.193	0.371*	0.197	0.380*	−0.219
Wood density	−0.186 ($n = 61$)	−0.215 ($n = 51$)	0.349** ($n = 79^{\S}$)	0.258 ($n = 64$)	−0.565*** ($n = 80^{\S}$)	−0.433** ($n = 64$)

Uncorr., correlations not corrected for phylogenetic effects; PIC, correlations calculated using phylogenetically independent contrasts; diam., diameter; FWTI%, fiber wall thickness index. Coefficients are statistically significant (*, $\alpha = 0.05$; **, $\alpha = 0.01$; ***, $\alpha = 0.001$) after correcting for false discovery rate in multiple comparisons using the Benjamini and Hochberg procedure [Benjamini Y, Hochberg Y (1995) Controlling the false discovery rate: A practical and powerful approach to multiple testing. *J R Stat Soc B* 57:289–300].

†Log-transformed.

‡Except for the bottom row, where different sample sizes are noted.

§Each of five species occurred at two sample sites.

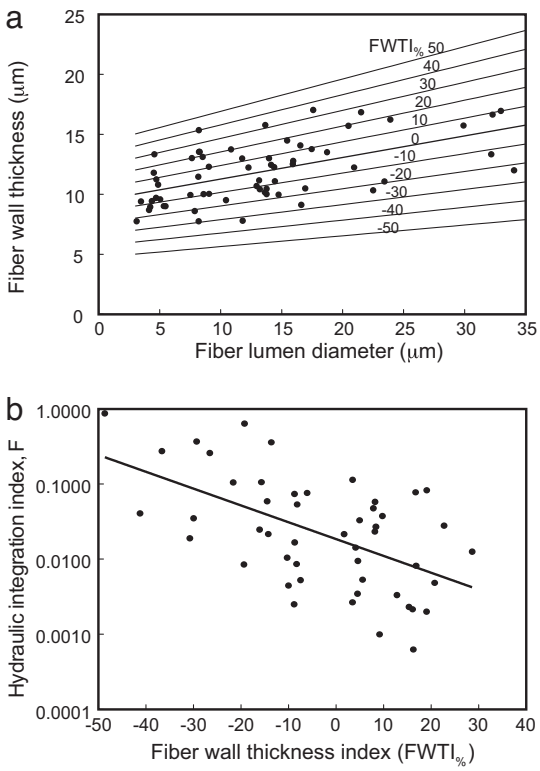

Fig. 4. FWTI%. (*a*) Relationship between fiber lumen diameter (FLD) and fiber wall thickness (FWT): FWTI% = 100 (1 − (0.1798 FLD + 9.4779)/FWT) (n = 62; r^2 = 0.319; $P < .0001$). The fiber wall thickness index FWTI% is the coefficient of variation of regression residuals, which is indicated by the thin, labeled lines. (*b*) Relationship between FWTI% and the hydraulic integration index F (n = 49; r^2 = 0.301; $P < .0001$).

causing asymmetric growth of the basal stem, as reported by Jones and Lord (23). However, partial dieback and differential branch growth are themselves a consequence of a lack of water sharing among branches and therefore indicate a preexisting modularity. Furthermore, uneven cambial activity preceding eventual stem segmentation begins, at least in some species, when plants are very small, before observed branch die back (23). Could stem segmentation be related to stem mechanics rather than aridity, such that tall shrubs may require round stems for mechanical support, whereas stems of smaller shrubs can split because they do not require much support? The answer is that stem segmentation is significantly related to aridity even when biomechanical constraints associated with increased height are taken into account. Moreover, stem segmentation does not seem to occur in small shrubs from wet environments but does occur in some tall desert shrubs, such as *Larrea tridentata*, which can reach heights of 3.5 m (37).

Could it be that a low degree of hydraulic integration, rather than being a drought adaptation itself, is associated with other structural adaptations that make a hydraulic system resistant to failure? According to the most recent theories about cavitation resistance (12–16), the answer seems to be that hydraulic integration and other structural adaptations are inseparably linked. The connectivity among angiosperm vessels, whether resulting from the number and size of intervessel pits (13) or from the architectural connectedness among vessels (12, 14), is thought to be a crucial adaptation that enables plants to minimize spread of emboli between vessels (12–16). In fact, vulnerability of plant organs to cavitation, as measured by the dehydration, air-injection, or centrifuge methods (38), may be related less to the resistance of individual water-filled xylem conduits to form emboli via wall collapse or air seeding from surrounding intercellular air spaces or gas-filled fibers than to the ability of gas to spread among vessels (12–15). At the organ level, what has been termed "cavitation resistance" in the literature (e.g., 7, 13, 15) probably is better characterized as a combination of resistance and redundancy, namely the resistance of the individual xylem conduits to forming emboli and the degree and type of redundancy of the conduit network (12, 14, 16).

Angiosperm shrubs seem to have evolved two independent ways of building a modular hydraulic system. Through asymmetric secondary growth that leads to fluted sapwood and in some cases to axis splitting (17, 22, 23), plants ensure complete hydraulic isolation of segments. This type of growth is associated with high wood density (Tables 2 and 3), with high implosion resistance of vessels, and therefore probably with high resistance to forming embolisms (6, 7). An alternative strategy to reduce the degree of hydraulic integration seems to be making fewer and larger vessels and surrounding them with a matrix of thick-walled, nonconducting, and possibly gas-filled fibers (25). For plants growing in very dry environments there may be a tradeoff between these two ways of achieving hydraulic modu-

Table 3. Comparison of structural and functional differences in shrub species from dry environments (MAP < 700 mm, AI < 0.6) that have completely split basal stems and species from the same environments that have non-splitting stems

	Species with nonsplitting stems			Species with split basal stems			
Trait	n	mean	SE	n	Mean	SE	P
Stem segmentation, S	27	1.3	0.1	14	3.2	0.3	***
Hydraulic integration, F	21	0.042	0.018	10	0.027	0.008	ns
Hydraulic integration, F, adjusted for split stems†	21	0.042	0.018	10	0.053	0.016	ns
Vessel density, mm^{-2}	27	69.7	6.8	14	95.0	11.2	*
Vessel hydraulic diam., μm	27	55.8	3.0	14	45.8	2.5	*
Fiber wall thickness, μm	27	11.6	0.5	14	11.7	0.6	ns
Fiber lumen diam., μm	27	11.6	1.3	14	9.4	1.5	ns
FWTI%	27	−2.57	3.4	14	2.1	3.3	ns
Fiber wall area, %	27	42.5	2.8	14	49.1	3.1	ns
Fiber lumen area, %	27	12.1	1.9	14	8.5	1.7	ns
$(t/b)_n^2$	27	0.030	0.003	13	0.047	0.007	***
Wood density, $g \cdot cm^{-3}$	27	0.69	0.02	14	0.78	0.04	*

AI, aridity index; FWTI%, fiber wall thickness index; MAP, mean annual precipitation; ns, not significant. Coefficients are statistically significant (*, $\alpha = 0.05$; ***, $\alpha = 0.001$) after correcting for false discovery rate in multiple comparisons using the Benjamini and Hochberg procedure [Benjamini Y, Hochberg Y (1995) Controlling the false discovery rate: A practical and powerful approach to multiple testing. *J R Stat Soc B* 57:289–300]. ns, Not significant.
†Hydraulic integration index F calculated only for the individual stem segment(s) that contained dye tracer.

larity. In vessel-bearing angiosperms, high resistance to embolism formation and vessel implosion is achieved by lowering vessel diameters (13) and increasing the wall-to-lumen ratio of vessels (7). Because hydraulic conductivity of capillaries is proportional to the fourth power of the capillary radius (1), a decrease in vessel diameters must be offset by a concomitant increase in vessel numbers to limit loss in conductivity. Asymmetric secondary growth may be a way to reduce the connectivity among vessels in species with small vessel diameters and high vessel densities (Table 3). High wood density may be a biomechanical requirement for shrubs that have partially or completely segmented stems and therefore lack the mechanical support provided by thicker stems with a core of heartwood. This group includes many of the most cavitation-resistant species from such genera as *Ceanothus*, *Adenostoma*, *Artemisia*, and *Larrea* (7, 39).

The implications of modular hydraulic systems for plant function are numerous. Hydraulic isolation of conduits could allow embolism repair while other parts of the xylem are under tension (10). Under drought conditions, when partial canopy dieback is a frequent occurrence in shrubs (40, 41), hydraulically isolated plant modules with some access to small pockets of water in heterogeneous soil may be able to survive if they are protected from sharing that water with drought-stressed modules (20). In contrast, frost, which also can induce vessel cavitation, is more likely to affect the whole plant equally (42); therefore hydraulic modularity probably does not provide benefits for resistance to or repair of frost-induced embolisms.

Modular hydraulic systems also reduce the spread of runaway embolisms, allow independent stomatal regulation of water use in hydraulic modules, and may help reduce water loss through hydraulic redistribution by restricting flow from one part of the root system to another. In environments not affected by frequent droughts, hydraulic integration seems to be advantageous to shrubs because it allows water and nutrient sharing among modules and rerouting of water flow around pathways blocked by tyloses or pathogens. Most trees in humid forests possess integrated hydraulic systems (31), although both vessel distribution (11) and phylogeny (43) can affect the degree of integration. Hydraulic integration is a trait with important implications for plant structure and function. Highly modular hydraulic systems correlate with the growth form, anatomy, and function of shrubs in dry environments, suggesting that modular hydraulic redundancy is an important, but hitherto largely overlooked, drought adaptation.

Materials and Methods

Field sites were located along transcontinental aridity gradients in North and South America between 31° and 35° latitude (Table 1). Climate data were obtained from nearby weather stations, and mean annual potential evapotranspiration was estimated using a global database (44, 45). At each site, shrubs were sampled during the active growing season using a randomized selection protocol that caused abundant shrub species to have a higher chance of being sampled than less abundant ones. Only healthy shrubs without evidence of partial canopy dieback were sampled. (For a list of species and numbers of individuals sampled at each site see the Table S1) For each shrub, a single, lateral woody root (∅ 2 to 11 mm) was excavated, cut under water, and inserted into a vial containing Acid Fuchsin dye (0.5%). After 1 day, the shrub was cut just below the main branching point, and the basal stem/root crown was taken to the laboratory for analysis of shape and dye-tracer distribution and for measurements of sapwood density and sapwood anatomy. Transverse sections of the basal stem at its most compact point were photographed, and the images were analyzed using SigmaScan Pro software, version 5.0 (SYSTAT Software Inc.).

Shrub growth forms were characterized by measurements of canopy height and widths, height-to-width ratios, canopy volume (calculated as an ellipsoid), and the height of the lowest branch above ground. The degree of physical segmentation of shrubs was characterized by the relationship between cross-sectional area and perimeter of the basal stem's living sapwood and associated undecayed heartwood at the basal stem's most compact point using the formula $S = p\sqrt{\pi}/(\sqrt{A}2\pi)$, with p = stem perimeter, A = basal stem cross-sectional area, and $S = 1$ for a circular area. The degree of hydraulic integration within the basal stem was characterized by measuring the fraction of basal stem cross-sectional area (without bark) colored by Acid Fuchsin dye and calculating a hydraulic integration index as $F = d / A$, with d = area of stem cross-section colored by dye and A = the total area of the basal cross section. Visual distinction between sapwood and heartwood was not possible for many of the species studied, and dye-based methods could not be used without affecting the distribution of Acid Fuchsin dye within the sample. Therefore the total cross-sectional stem area was used to calculate F, and possible effects of total stem area on F were accounted for statistically (as described later). Parameters S and F were log-transformed to meet normality requirements and were analyzed statistically in general linear models as functions of MAP and transect location (North or South America) using SYSTAT software, version 12 . To account for possible effects of biomechanics on the relationship between stem segmentation and aridity, parameter S also was analyzed in a general linear model with MAP, shrub height, and their interaction included as variables. To account for effects of the cross-sectional stem area on parameter F, this parameter also was analyzed in a general linear model with MAP, stem area, and their interaction included as variables.

Sapwood samples from basal stems for analyses of wood anatomy and wood density were softened by boiling and were sectioned and stained. Images of ≈3 mm^2 of transverse sections of sapwood were analyzed in ArcView, version 3.2 (ESRI). Using a drawing tablet, 200 fibers (including libriform fibers and fiber-tracheids) were drawn and measured for wall thickness (FWT) and fiber lumen diameter (FLD), and the entire image was used to determine vessel density, mean vessel hydraulic diameter (46), and the percentages of areas occupied by fiber lumens (FLA) and walls (FWA). A fiber wall thickness index ($FWTI_{\%}$), which included a correction for the relationship between FLD and FWT, was calculated as the coefficient of variation of the residuals of a linear regression of FWT as function of FLD. The theoretical implosion resistance of vessels based on the squared wall thickness-to-span ratio of vessels $(t/b)_h^2$ was measured as described by Hacke *et al.* (7). Sapwood density in basal stems was measured using the Archimedes principle (47). Anatomical traits and wood density were analyzed for their correlation to MAP, the integration index F, and stem segmentation index S. Relationships between non-normally distributed traits were analyzed using Wilcoxon signed rank tests. Linear correlations were calculated for uncorrected trait values and for PICs to account for phylogenetic effects. PICs were calculated using PDAP:PDTREE (48), a module of Mesquite (version 1.1) (49), and Phylomatic (50) was used to generate an initial tree. Most remaining polytomies were resolved using published phylogenies (51–58), leaving only a few unresolved. Any anatomical trait that had a significant association between the absolute value of its standardized independent contrast versus its standard deviation (59–61) was log-transformed (FLD and FWT) or arsine-transformed (FLA and FWA). All branch lengths were set to 1. Statistical significance of correlations was determined in two-tailed tests after correcting for false discovery rate in multiple comparisons using the Benjamini and Hochberg procedure (62, 63).

ACKNOWLEDGMENTS. We thank Greg Pongetti, Daisha Ortega, Fernando Biganzoli, Andrés Rolhauser, Sarina Lambert, Maya Mazon, and Pauline Grierson for help with the field work. We thank Esteban Jobbágy, Lisa Donovan, Robert B. Jackson, Brian D. Kloeppel, Jim Ansley, and Mary Morrison for hosting site visits and Nicandro ''Cano'' Agüero for permission to conduct research on his land. Very helpful comments on the manuscript from two anonymous reviewers are gratefully acknowledged. Funding for this research was provided by a grant from the Andrew W. Mellon Foundation to H.J.S.

1. Tyree MT, Zimmermann MH (2002) *Xylem Structure and the Ascent of Sap* (Springer-Verlag, Berlin).
2. Zwieniecki MA, Hutyra L, Thompson MV, Holbrook NM (2000) Dynamic changes in petiole specific conductivity in red maple (*Acer rubrum* L.), tulip tree (*Liriodendron tulipifera* L.) and northern fox grape (*Vitis labrusca* L.). *Plant Cell Environ* 23:407–414.
3. Domec JC, *et al.* (2006) Diurnal and seasonal variation in root xylem embolism in neotropical savanna woody species: Impact on stomatal control of plant water status. *Plant Cell Environ* 29:26–35.
4. McCully ME, Huang CX, Ling LEC (1998) Daily embolism and refilling of xylem vessels in the roots of field-grown maize. *New Phytol* 138:327–342.
5. Tyree MT, Sperry JS (1988) Do woody plants operate near the point of catastrophic xylem dysfunction caused by dynamic water stress? Answers from a model. *Plant Physiol* 88:574–580.
6. Jacobsen AL, Ewers FW, Pratt RB, Paddock WA III, Davis SD (2005) Do xylem fibers affect vessel cavitation resistance? *Plant Physiol* 139:546–556.
7. Hacke UG, Sperry JS, Pockman WT, Davis SD, McCulloh KA (2001) Trends in wood density and structure are linked to prevention of xylem implosion by negative pressure. *Oecologia* 126:457–461.
8. Salleo S, Lo Gullo MA, Trifilò P, Nardini A (2004) New evidence for a role of vessel-associated cells and phloem in the rapid xylem refilling of cavitated stems of *Laurus nobilis* L. *Plant Cell Environ* 27:1065–1076.

9. Tyree MT, Salleo S, Nardini A, Lo Gullo MA, Mosca R (1999) Refilling of embolized vessels in young stems of laurel. Do we need a new paradigm? *Plant Physiol* 120:11–21.
10. Clearwater MJ, Goldstein G (2005) in *Vascular Transport in Plants*, eds. Holbrook NM, Zwieniecki MA. (Elsevier Academic, Amsterdam), pp. 375–399.
11. Zanne AE, Sweeney KP, Sharma M, Orians CM (2006) Patterns and consequences of differential vascular sectoriality in 18 temperate tree and shrub species. *Funct Ecol* 20:200–206.
12. Loepfe L, Martienez-Vilalta J, Piñol J, Mencuccini M (2007) The relevance of xylem network structure for plant hydraulic efficiency and safety. *J Theor Biol* 247:788–803.
13. Hacke UG, Sperry JS, Wheeler JK, Castro L (2006) Scaling of angiosperm xylem structure with safety and efficiency. *Tree Physiol* 26:689–701.
14. Ewers FW, Ewers JM, Jacobsen AL, López-Portillo J (2007) Vessel redundancy: Modeling safety in numbers. *IAWA J* 28:373–388.
15. Wheeler JK, Sperry JS, Hacke UG, Huang N (2005) Inter-vessel pitting and cavitation in woody Rosaceae and other vesseled plants: a basis for a safety vs. efficiency trade-off in xylem transport. *Plant Cell Environ* 28:800–812.
16. Choat B, Cobb AR, Jansen S (2008) Structure and function of bordered pits: New discoveries and impacts on whole-plant hydraulic function. *New Phytol* 177:608–626.
17. Schenk HJ (1999) Clonal splitting in desert shrubs. *Plant Ecol* 141:41–52.
18. Smith DJ (2005) *Reliability, Maintainability and Risk: Practical Methods for Engineers Including Reliability Centred Maintenance and Safety-Related Systems* (Elsevier Butterworth-Heinemann, Oxford, United Kingdom).
19. Wunderlich WO (2004) *Hydraulic Structures: Probabilistic Approaches to Maintenance* (American Society of Civil Engineers, Reston, VA).
20. Jones CS (1984) The effect of axis splitting on xylem pressure potentials and water-movement in the desert shrub *Ambrosia dumosa* (Gray) Payne (Asteraceae). *Bot Gaz* 145:125–131.
21. Keeley JE (1975) Longevity of nonsprouting *Ceanothus*. *Am Midl Nat* 93:504–507.
22. Ginzburg C (1963) Some anatomic features of splitting of desert shrubs. *Phytomorphol* 13:92–97.
23. Jones CS, Lord EM (1982) The development of split axes in *Ambrosia dumosa* (Gray) Payne (Asteraceae). *Bot Gaz* 143:446–453.
24. Ellmore GS, Zanne AE, Orians CM (2006) Comparative sectoriality in temperate hard-woods: hydraulics and xylem anatomy. *Bot J Linnean Soc* 150:61–71.
25. Carlquist S (1984) Vessel grouping in dicotyledon wood: significance and relationship to imperforate tracheary elements. *Aliso* 10:505–525.
26. Umebayashi T, *et al*. (2007) Optimal conditions for visualizing water-conducting pathways in a living tree by the dye injection method. *Tree Physiol* 27:993–999.
27. Utsumi Y, Sano Y, Fujikawa S, Funada R, Ohtani J (1998) Visualization of cavitated vessels in winter and refilled vessels in spring in diffuse-porous trees by cryo-scanning electron microscopy. *Plant Physiol* 117:1463–1471.
28. Utsumi Y, Sano Y, Funada R, Fujikawa S, Ohtani J (1999) The progression of cavitation in earlywood vessels of *Fraxinus mandshurica* var *japonica* during freezing and thaw-ing. *Plant Physiol* 121:897–904.
29. Sano Y, Okamura Y, Utsumi Y (2005) Visualizing water-conduction pathways of living trees: selection of dyes and tissue preparation methods. *Tree Physiol* 25:269–275.
30. Orians CM, Van Vuuren MMI, Harris NL, Babst BA, Ellmore GS (2004) Differential sectoriality in long-distance transport in temperate tree species: evidence from dye flow, ^{15}N transport, and vessel element pitting. *Trees* 18:501–509.
31. Waisel Y, Liphschitz N, Kuller Z (1972) Patterns of water movement in trees and shrubs. *Ecology* 53:520–523.
32. Jacobsen AL, Pratt RB, Ewers FW, Davis SD (2007) Cavitation resistance among 26 chaparral species of southern California. *Ecol Monogr* 77:99–115.
33. Royer DL, Wilf P, Janesko DA, Kowalski EA, Dilcher DL (2005) Correlations of climate and plant ecology to leaf size and shape: potential proxies for the fossil record. *Amer J Bot* 92:1141–1151.
34. Ehleringer, J (1980) in *Adaptations of plants to water and high temperature stress*, eds. Turner NC. Kramer PJ. (Wiley–Interscience, New York), pp. 295–308.
35. Wright IJ, *et al*. (2004) The worldwide leaf economics spectrum. *Nature* 428:821–827.
36. Ehleringer JR, Monson RK (1993) Evolutionary and ecological aspects of photosynthetic pathway variation. *Ann Rev Ecol Syst* 24:411–439.
37. Turner RM, Bowers JE, Burgess TL (1995) *Sonoran Desert Plants: An Ecological Atlas* (The University of Arizona Press, Tucson).
38. Alder NN, Pockman WT, Sperry JS, Nuismer SM (1997) Use of centrifugal force in the study of xylem cavitation. *J Exp Bot* 48:665–674.
39. Jacobsen AL, Pratt RB, Davis SD, Ewers FW (2007) Cavitation resistance and seasonal hydraulics differ among three arid Californian plant communities. *Plant Cell Environ* 30:1599–1609.
40. Orshan G, Zand G (1962) Seasonal body reduction of certain desert halfshrubs. *Bull Res Counc of Israel* 11D:35–42.
41. Davis SD, *et al*. (2002) Shoot dieback during prolonged drought in *Ceanothus* chaparral of California: a possible case of hydraulic failure. *Amer J Bot* 89:820–828.
42. Boorse GC, Ewers FW, Davis SD (1998) Response of chaparral shrubs to below-freezing temperatures: acclimation, ecotypes, seedlings vs. adults. *Amer J Bot* 85:1224–1230.
43. Orians CM, Babst BB, Zanne AE (2005) in *Vascular Transport in Plants*, eds. Holbrook NM, Zwieniecki MA. (Elsevier/AP co-imprint, Oxford).
44. Choudhury BJ (1997) Global pattern of potential evaporation calculated from the Penman-Monteith equation using satellite and assimilated data. *Remote Sens Environ* 61:64–81.
45. Choudhury BJ, DiGirolamo NE (1998) A biophysical process-based estimate of global land surface evaporation using satellite and ancillary data. I. Model description and comparison with observations. *J Hydrol* 205:164–185.
46. Kolb KJ, Sperry JS (1999) Transport constraints on water use by the Great Basin shrub, *Artemisia tridentata*. *Plant Cell Environ* 22:925–935.
47. Hacke UG, Sperry JS, Pittermann J (2000) Drought experience and cavitation resistance in six shrubs from the Great Basin, Utah. *Basic Appl Ecol* 1:31–41.
48. Midford PE, Garland T, Jr., Maddison WP (2005) PDAP package of Mesquite, version 1.06. Available at: http://mesquiteproject.org/PDAP_mesquite/. Accessed July 18, 2008.
49. Maddison WP, Maddison DR (2004) Mesquite: a modular system for evolutionary analysis. Version 1.05. Available at: http://mesquiteproject.org. Accessed July 18, 2008.
50. Webb CO, Donoghue MJ (2005) Phylomatic: Tree assembly for applied phylogenetics. *Mol Ecol Notes* 5:181–183.
51. Floyd JW (2002) Phylogenetic and biogeographic patterns in *Gaylussacia* (Ericaceae) based on morphological, nuclear DNA, and chloroplast DNA variation. *Syst Bot* 27:99–115.
52. Goertzen LR, Cannone JJ, Gutell RR, Jansen RK (2003) ITS secondary structure derived from comparative analysis: implications for sequence alignment and phylogeny of the Asteraceae. *Mol Phylogen Evol* 29:216–234.
53. Lia VV, Confalonieri VA, Comas CI, Hunziker JH (2001) Molecular phylogeny of *Larrea* and its allies (Zygophyllaceae): Reticulate evolution and the probable time of Creosote Bush arrival to North America. *Moc Phylogen Evol* 21:309–320.
54. Martins TR, Barkmani TJ (2005) Reconstruction of Solanaceae phylogeny using the nuclear gene SAMT. *Syst Bot* 30:435–447.
55. Olmstead RG, Palmer JD (1992) A chloroplast DNA phylogeny of the Solanaceae: subfamilial relationships and character evolution. *Ann Miss Bot Gard* 79:346–360.
56. Urbatsch LE, Baldwin BG, Donoghue MJ (2000) Phylogeny of the coneflowers and relatives (Heliantheae: Asteraceae) based on nuclear rDNA internal transcribed spacer (ITS) sequences and chloroplast DNA restriction site data. *Syst Bot* 25:539–565.
57. Urbatsch LE, Roberts R, Karaman V (2003) Phylogenetic evaluation of *Xylothamia*, *Gundlachia* and related genera (Asteraceae, Astereae) based on ETS and ITS NRDNA sequence data *Amer J Bot* 90:634–649.
58. Wojciechowski MF, Lavin M, Sanderson JS (2004) A phylogeny of legumes (Leguminosae) based on analysis of the plastid MATK gene resolves many well-supported subclades within the family. *Amer J Bot* 91:1846–1862.
59. Garland T, Jr, Huey RB, Bennett AF (1991) Phylogeny and thermal physiology in lizards: a reanalysis. *Evolution* 45:1969–1975.
60. Garland T, Jr, Harvey PH, Ives AR (1992) Procedures for the analysis of comparative data using phylogenetically independent contrasts. *Syst Biol* 41:18–32.
61. Garland T, Jr, Janis CM (1993) Does metatarsal/femur ratio predict maximal running speed in cursorial mammals? *J Zool* 229:133–151.
62. Benjamini Y, Hochberg Y (1995) Controlling the false discovery rate: A practical and powerful approach to multiple testing. *J R Stat Soc B* 57:289–300.
63. Verhoeven KJF, Simonsen KL, McIntyre LM (2005) Implementing false discovery rate control: Increasing your power. *Oikos* 108:643–647.